Available online at www.sciencedirect.com
SCIENCE DIRECT®
International Journal of Thermal Sciences 45 (2006) 419–432
International Journal of Thermal Sciences
www.elsevier.com/locate/ijts

Simplified building model for transient thermal performance estimation using GA-based parameter identification

Shengwei Wang *, Xinhua Xu

Department of Building Services Engineering, The Hong Kong Polytechnic University, Kowloon, Hong Kong

Received 30 March 2005; received in revised form 21 June 2005; accepted 21 June 2005

Available online 19 August 2005

Abstract

Building simple and effective models are essential to many applications, such as building performance diagnosis and optimal control. Detailed physical models are time consuming and often not cost-effective. Black box models require large amount of training data and may not always reflect the physical behaviors. In this study, a method is proposed to simplify the building thermal model and to identify the parameters of the simplified model. For building envelopes, the model parameters can be determined using the easily available physical details based on the frequency characteristic analysis. For the building internal mass involving various components, it is very difficult to obtain the detailed physical properties. To overcome this problem, the building internal mass is represented by a thermal network of lumped thermal mass and the parameters are identified using operation data. Genetic algorithm (GA) estimators are developed to identify these parameters. The simplified dynamic building energy model is validated on a real commercial office building in different weather conditions.

Keywords: Simplified model; Thermal performance; Parameter identification; Frequency characteristic analysis; Genetic algorithm

1. Introduction

Excessive energy is consumed in buildings and HVAC systems because they often fail to operate as intended, after a period of operation even with correct commissioning [1,2]. Comfort problems often occur simultaneously. These failures may be due to inappropriate temperature set points as well as inappropriate fresh air intake, etc. Proper operation of the building system can lead to improved occupant comfort and health, improved energy efficiency, longer life cycle of equipments, reduced maintenance costs, and reduced unscheduled equipment shut down time, etc. Normally, the Kilowatt meter is always needed to measure the total electricity consumption at the building level and the cooling/heating energy consumption can often be measured at the central plant. They provide information for performance evaluation, fault detection and diagnosis, etc. However, baseline energy consumption is often needed for reference for such purposes. In order to predict the overall energy consumption for reference, it is fundamental to have a model to estimate the cooling or heating energy consumption to maintain temperature and humidity of the air in the building [3–5]. Viewing the building system as a whole, many researchers have developed different reference models for applications, which can be mainly categorized into physical models, data driven models and gray models.

Available simulation models such as EnergyPlus [6] and DOE-2 [7] etc., are typical detailed physical models. However, the calibration process of the simulation models is a great challenge. A large number of parameters are needed as inputs for simulation, and the process of collecting physical descriptions is time consuming and probably does not cost effective. Experiences of some researchers show that differences of 50% or more between the simulation results based on design data and the measured consumption are not unusual [8]. Dynamic data driven models are capable of capturing dynamics such as mass dynamics to some extends and better suited to handle inter-correlated forcing functions or independent parameters [9–11]. However,

* Corresponding author.
E-mail address: beswwang@polyu.edu.hk (S. Wang).

1290-0729/$ – see front matter
doi:10.1016/j.ijthermalsci.2005.06.009

Nomenclature

A, B, C, D	transmission matrix element	
a	thermal diffusivity	
b, c, d	CTF coefficients	
C	thermal capacitance	$J{\cdot}m^{-2}{\cdot}K^{-1}$
C_P	specific heat	$J{\cdot}kg^{-1}{\cdot}K^{-1}$
d_f	difference between the two maximum fitness values	
f	fitness function	
G	s-transfer function	
J	objective function	
L	thickness	m
M	transmission matrix	
N	number of frequency points	
PL	phase lag	rad
Q	cooling/heating load or heat	kW
q	heat flow	$W{\cdot}m^{-2}$
R	thermal resistance	$m^2{\cdot}K{\cdot}W^{-1}$
s	Laplace variable or roots	
T	air temperature	°C or K
t	time	second or hour
W	Weighting factor	
$\lvert\cdot\rvert$	amplitude or absolute value	$W{\cdot}m^{-2}{\cdot}K^{-1}$
$\sum$	summation	

Greek symbols

λ	thermal conductivity	$W{\cdot}m^{-1}{\cdot}K^{-1}$
ρ	density	$kg{\cdot}m^{-3}$
ω	frequency	$rad{\cdot}s^{-1}$
ε_f	threshold value	

Superscripts

$'$	associated with simplified 3R2C model
AM	associated with amplitude of frequency characteristic
PL	associated with phase lag of frequency characteristic

Subscripts

act	actual cooling load
conv	convective heat
ei	associated with external wall at the ith orientation
est	estimated
fr	fresh air
im	associated with building internal mass
in	inside, indoor air
la	latent heat
out	outside
r	associated with radiation
rf	associated with roof
rtn	return air
sol	associated with solar air temperature
win	window
X, Y, Z	associated with external, across and internal heat conduction

it is generally necessary to acquire data over a long period of time with widely varying conditions in order to train the models for accurate predictions under all conditions.

Gray models assume the physical structure and their parameters have definite physical meanings. The parameters can be backed out with operation data. Braun and Chaturvedi [12] developed an inverse gray thermal network model for transient building load prediction. Liao and Dexter [13] developed a gray second-order physical model to simulate the dynamic behavior of the existing heating system of a residential building with multi-zone. The gray models can predict long-term energy performance with short term operation data monitoring. Although gray models can represent the physical properties of building system and predict energy consumption, some easily available building information can be utilized to enhance the simplified models and reduce the number of parameters to be identified with operation data.

This paper presents a method to simplify building models and identify their parameters using easily available building physical properties and short-term operation data monitored. The simplified building model (namely simplified building energy model in this paper) consists of the simplified models of the building envelopes and the simplified model of the building internal mass. The properties of the building envelopes are relatively easily available to establish the simplified models of the building envelopes. 3R2C models are usually utilized to simulate the building envelopes [12,14]. The nodal placement of the 3R2C model can be obtained by matching the theoretical frequency response characteristics of the building envelope with the frequency response characteristics of the simplified model using genetic algorithm [15]. Building internal mass, such as internal structures, partitions, carpet and furniture etc., is difficult to obtain. They are represented with lumped thermal internal mass of a 2R2C model. The parameters of the simplified 2R2C model of the building internal mass can be identified with operation data after the simplified models of the building envelopes have been obtained. As the model validation, the simplified building energy model of a real commercial office building was established on the basis of the operation data in short period time. The model was then verified in various other operation conditions. The results show that the established simplified building energy model can predict thermal performance with good accuracy and robustness.

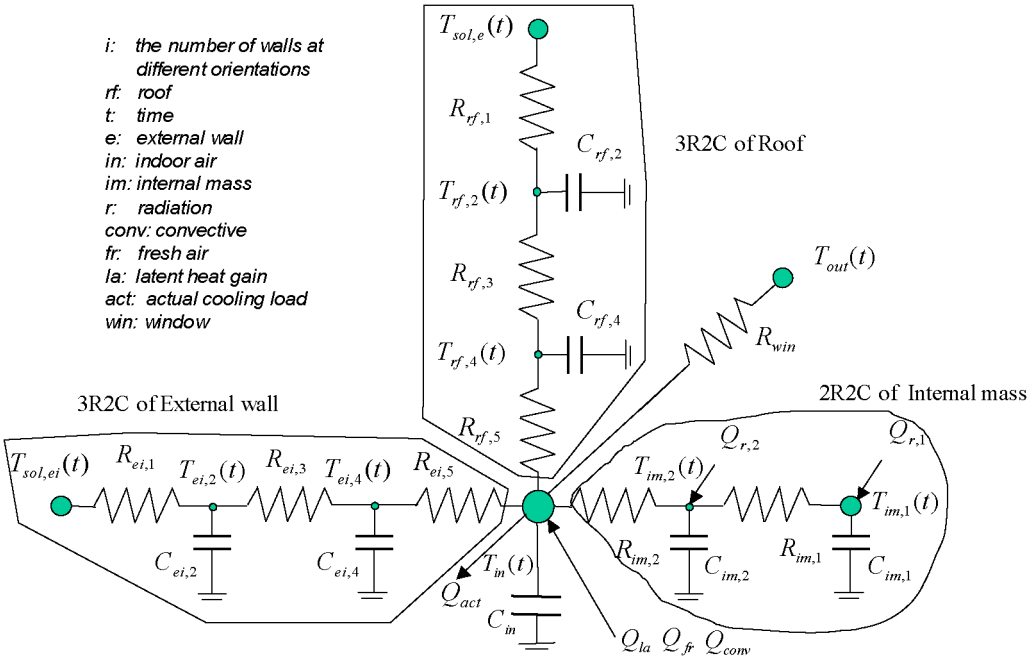

Fig. 1. Schematics of the simplified building energy model.

2. A brief on simplified building energy modeling

Fig. 1 illustrates the simplified building energy model. Building physical properties affecting thermal transfer are mainly those of the building envelopes and internal mass. They are handled separately. Building envelopes are mainly external walls and roof(s). External walls should be considered respectively according to the orientations because the dynamic models of the external walls at different orientations have different forcing functions due to the changing position of the sun. External walls and ceiling/roof are simplified as 3R2C models, respectively. Building internal mass includes floors, partitions, crawl space in ceiling, internal walls, and furniture etc. It absorbs radiant heat through the windows and that from occupants, lighting, and equipments etc., and then releases (or absorbs) the heat gradually to the air space. The building internal mass is represented with a 2R2C model, which consists of two resistances and two capacitances, as shown in Fig. 1. All resistances and capacitances are assumed to be time invariant. The windows have negligible energy storage and are represented with a pure resistance (R_{win}). The effect of varying wind velocity on external wall convection coefficients is not considered.

The whole building energy consumption can be represented with the following differential equations:

$$C_{\text{rf},2}\frac{\mathrm{d}T_{\text{rf},2}(t)}{\mathrm{d}t} = \frac{T_{\text{sol,rf}}(t) - T_{\text{rf},2}(t)}{R_{\text{rf},1}} - \frac{T_{\text{rf},2}(t) - T_{\text{rf},4}(t)}{R_{\text{rf},3}} \tag{1}$$

$$C_{\text{rf},4}\frac{\mathrm{d}T_{\text{rf},4}(t)}{\mathrm{d}t} = \frac{T_{\text{rf},2}(t) - T_{\text{rf},4}(t)}{R_{\text{rf},3}} - \frac{T_{\text{rf},4}(t) - T_{\text{in}}(t)}{R_{\text{rf},5}} \tag{2}$$

$$C_{\text{ei},2}\frac{\mathrm{d}T_{\text{ei},2}(t)}{\mathrm{d}t} = \frac{T_{\text{sol,ei}}(t) - T_{\text{ei},2}(t)}{R_{\text{ei},1}} - \frac{T_{\text{ei},2}(t) - T_{\text{ei},4}(t)}{R_{\text{ei},3}} \tag{3}$$

$$C_{\text{ei},4}\frac{\mathrm{d}T_{\text{ei},4}(t)}{\mathrm{d}t} = \frac{T_{\text{ei},2}(t) - T_{\text{ei},4}(t)}{R_{\text{ei},3}} - \frac{T_{\text{ei},4}(t) - T_{\text{in}}(t)}{R_{\text{ei},5}} \tag{4}$$

$$C_{\text{im},1}\frac{\mathrm{d}T_{\text{im},1}(t)}{\mathrm{d}t} = Q_{r,1} - \frac{T_{\text{im},1}(t) - T_{\text{im},2}(t)}{R_{\text{im},1}} \tag{5}$$

$$C_{\text{im},2}\frac{\mathrm{d}T_{\text{im},2}(t)}{\mathrm{d}t} = Q_{r,2} + \frac{T_{\text{im},1}(t) - T_{\text{im},2}(t)}{R_{\text{im},1}} - \frac{T_{\text{im},2}(t) - T_{\text{in}}(t)}{R_{\text{im},2}} \tag{6}$$

$$Q_{\text{est}} = \sum_{i=1}^{n}\left(\frac{T_{\text{ei},4}(t) - T_{\text{in}}(t)}{R_{\text{ei},5}}\right) + \frac{T_{\text{rf},4}(t) - T_{\text{in}}(t)}{R_{\text{rf},5}} + \frac{T_{\text{im},2}(t) - T_{\text{in}}(t)}{R_{\text{im},2}} + \frac{T_{\text{out}}(t) - T_{\text{in}}(t)}{R_{\text{win}}} - C_{\text{in}}\frac{\mathrm{d}T_{\text{in}}(t)}{\mathrm{d}t} + (Q_{\text{conv}} + Q_{\text{fr}} + Q_{\text{la}}) \tag{7}$$

where, C and R are resistance and capacitance, T is temperature, subscript rf, im, ei, win, and in, indicate roof, internal mass, the ith external wall, window and inside respectively. $Q_{\text{r},1}$ and $Q_{\text{r},2}$ absorbed by the nodes $C_{\text{im},1}$ and $C_{\text{im},2}$ respectively are the radiation which includes the radiation from solar radiation through windows, from occupants, lights etc. Q_{conv} is the convective heat from occupants, lights and equipments etc. Q_{fr} is the heat transfer because of fresh air induction, infiltration (exfiltration). Q_{la} is the latent heat

gain from occupants etc. Q_{est} is the model-estimated cooling load.

The properties of the building envelopes are relatively easy to obtain which can be utilized to establish the simplified 3R2C models of building envelopes. The parameters of 3R2C models of the building envelopes can be determined by comparing the theoretical frequency response characteristics of building envelopes with the frequency response characteristics of the simplified model using genetic algorithm, which is presented in Section 3 in detail. The parameter optimization of the 2R2C model of the building internal mass is described in Section 4.

3. Simplified models of the building envelopes of optimal parameters

The optimal nodal placement of simplified models of the building envelopes is based on the equivalent frequency characteristics of the simplified models and their relevant theoretical models. The process of the optimal nodal placement of simplified models of the building envelopes is to search the best parameters of the models allowing the frequency characteristics of the simplified model match that of the theoretical models the best. First, the theoretical frequency characteristic of heat transfer of the building envelope is deduced. Second, the frequency characteristic of the simplified model (3R2C models) is deduced. Then the objective function of parameter optimization is given with the deduced frequency characteristics. The GA estimator for parameter optimization of 3R2C models of the building envelopes as well as for the 2R2C model of the building internal mass is given in Section 5.

3.1. Theoretical frequency characteristics of heat transfer through constructions

The method to deduce the transmission matrix of heat transfer for one-dimensional homogeneous multilayer plane constructions in Laplace domain has been presented in many literatures [16–18]. The deduction process implemented in this study is briefed as follows.

The transmission equation (8), in terms of Laplace variable s, relates the temperatures and heat flows at both sides of the wall, which includes the surface films at both sides.

$$\begin{bmatrix} T_{\text{in}}(s) \\ q_{\text{in}}(s) \end{bmatrix} = M(s) \begin{bmatrix} T_{\text{out}}(s) \\ q_{\text{out}}(s) \end{bmatrix} = \begin{bmatrix} A(s) & B(s) \\ C(s) & D(s) \end{bmatrix} \begin{bmatrix} T_{\text{out}}(s) \\ q_{\text{out}}(s) \end{bmatrix} \tag{8}$$

where T is temperature, q is heat flow, $M(s)$ is the total transmission matrix of the entire wall, and also the products of individual layer transmission matrix including the surface films at both sides as follows:

$$M(s) = \begin{bmatrix} A(s) & B(s) \\ C(s) & D(s) \end{bmatrix} = M_{\text{in}}(s) M_n(s) \cdots M_1(s) M_{\text{out}}(s) \tag{9}$$

where

$$M_i(s) = \begin{bmatrix} A_i(s) & B_i(s) \\ C_i(s) & D_i(s) \end{bmatrix} \quad (i = 1, 2, \ldots, n). \tag{10}$$

The elements of all the layer transmission matrices can be given in hyperbolic function forms as shown in Eqs. (11)–(13):

$$A_i = D_i = \cosh(L_i \sqrt{s\rho_i C_{\text{P}i}/\lambda_i}) \tag{11}$$

$$B_i = -\sinh(L_i \sqrt{s\rho_i C_{\text{P}i}/\lambda_i})/(\lambda_i \sqrt{s\rho_i C_{\text{P}i}/\lambda_i}) \tag{12}$$

$$C_i = -\lambda_i \sqrt{s\rho_i C_{\text{P}i}/\lambda_i} \sinh(L_i \sqrt{s\rho_i C_{\text{P}i}/\lambda_i}) \tag{13}$$

where, λ, ρ and C_{P} are the thermal conductivity, density and specific heat respectively, i is the ith layer of the solid wall. When a layer has negligible heat capacitance compared to its thermal resistance (e.g., cavity layer, surface films), its layer transmission matrix becomes

$$M_i = \begin{bmatrix} 1 & -R_i \\ 0 & 1 \end{bmatrix} \tag{14}$$

where R_i is the thermal resistance of the cavity layers or surface films.

Thus, for the inside and outside surface films, the matrices are

$$M_{\text{in}}(s) = \begin{bmatrix} 1 & -R_{\text{in}} \\ 0 & 1 \end{bmatrix}, \qquad M_{\text{out}}(s) = \begin{bmatrix} 1 & -R_{\text{out}} \\ 0 & 1 \end{bmatrix} \tag{15}$$

where, R_{in} and R_{out} are the thermal resistance of the surface films of both the inside wall and outside wall respectively.

From Eq. (8), the transmission equation relating temperatures to heat flows on both sides is given by Eq. (16):

$$\begin{bmatrix} q_{\text{out}}(s) \\ q_{\text{in}}(s) \end{bmatrix} = \begin{bmatrix} -G_X(s) & G_Y(s) \\ -G_Y(s) & G_Z(s) \end{bmatrix} \begin{bmatrix} T_{\text{out}}(s) \\ T_{\text{in}}(s) \end{bmatrix} \tag{16}$$

where, $G_X(s)$, $G_Y(s)$ and $G_Z(s)$ are the transfer functions of external, cross and internal heat conduction of the construction, respectively. All of them are complicated transcendental hyperbolic functions, especially for a construction of more than two layers. Since $A(s)D(s) - B(s)C(s) = 1$, they can be expressed as Eqs. (17)–(19).

$$G_X(s) = A(s)/B(s) \tag{17}$$

$$G_Y(s) = 1/B(s) \tag{18}$$

$$G_Z(s) = D(s)/B(s) \tag{19}$$

Substituting s with $j\omega (j = \sqrt{-1})$ in Eqs. (17)–(19), one can yield the complex functions $G_X(j\omega)$, $G_Y(j\omega)$ and $G_Z(j\omega)$, which are the theoretical frequency characteristic of the external, cross and internal heat conduction, respectively [19]. These frequency characteristics are represented by the amplitudes and phase lags of these three complex functions representing the theoretical frequency characteristic of the external, cross and internal heat conduction, which are used as the reference of the frequency characteristics in optimization.

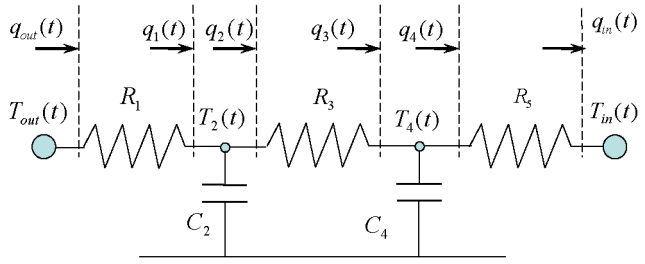

Fig. 2. Schematics of the simplified model of building envelope.

3.2. Frequency characteristics of heat transfer of simplified models

The building envelopes including external walls and roofs can be represented as 3R2C models using a uniform model of five elements (three resistances and two capacitances), as illustrated by Fig. 2. To calculate the frequency characteristics of the simplified models in the concerned frequency range, the transfer functions of the external, cross and internal heat conduction of simplified models are presented as follows.

The transmission equation (20) of the 3R2C model, in terms of Laplace variable s, relates the temperatures and heat flows at both sides of the wall, which includes the surface films at both sides.

$$\begin{bmatrix} T_{\text{in}}(s) \\ q_{\text{in}}(s) \end{bmatrix} = \begin{bmatrix} 1 & -R_5 \\ 0 & 1 \end{bmatrix} \begin{bmatrix} 1 & -R_3 \\ -C_4 s & C_4 R_3 s + 1 \end{bmatrix} \times \begin{bmatrix} 1 & -R_1 \\ -C_2 s & C_2 R_1 s + 1 \end{bmatrix} \begin{bmatrix} T_{\text{out}}(s) \\ q_{\text{out}}(s) \end{bmatrix} = \begin{bmatrix} A' & B' \\ C' & D' \end{bmatrix} \begin{bmatrix} T_{\text{out}}(s) \\ q_{\text{out}}(s) \end{bmatrix} \tag{20}$$

where

$$A' = 1 + (C_4 R_3 + C_2 R_3 + C_2 R_5) s + C_4 C_2 R_5 R_3 s^2 \tag{21}$$

$$B' = -(R_5 + R_3 + R_1) - (C_4 R_3 R_1 + C_2 R_3 R_1 + C_2 R_5 R_1 + C_4 R_5 R_3) s - C_4 C_2 R_5 R_3 R_1 s^2 \tag{22}$$

$$C' = -(C_4 + C_2) s - C_4 C_2 R_3 s^2 \tag{23}$$

$$D' = 1 + (C_4 R_1 + C_4 R_3 + C_2 R_1) s + C_4 C_2 R_3 R_1 s^2 \tag{24}$$

From Eq. (20), the transmission equation relating temperatures to heat flows on both sides of the 3R2C model is given by Eq. (25):

$$\begin{bmatrix} q_{\text{out}}(s) \\ q_{\text{in}}(s) \end{bmatrix} = \begin{bmatrix} -G'_X(s) & G'_Y(s) \\ -G'_Y(s) & G'_Z(s) \end{bmatrix} \begin{bmatrix} T_{\text{out}}(s) \\ T_{\text{in}}(s) \end{bmatrix} \tag{25}$$

where, $G'_X(s)$, $G'_Y(s)$ and $G'_Z(s)$ are the transfer functions of the external, cross and internal heat conduction of the 3R2C model of the construction respectively. All of them are the quotients of two polynomials respectively which can be expressed as Eqs. (26)–(28):

$$G'_X(s) = A'(s)/B'(s) \tag{26}$$

$$G'_Y(s) = 1/B'(s) \tag{27}$$

$$G'_Z(s) = D'(s)/B'(s) \tag{28}$$

Substituting s with $j\omega (j = \sqrt{-1})$ in Eqs. (26)–(28), one can yield the complex functions $G'_X(j\omega)$, $G'_Y(j\omega)$ and $G'_Z(j\omega)$, which are the frequency characteristics of the external, cross and internal heat conduction of the simplified 3R2C model, respectively. These frequency characteristics are represented also by the amplitudes and phase lags of these three complex functions representing the frequency characteristic of the external, cross and internal heat conduction of the simplified model, which are compared with the theoretical frequency characteristics in order to optimize their parameters.

3.3. Objective function of optimization

From the viewpoint of simplification [20], the simplified model should behave as the equivalent frequency response characteristics if it can represent the real system of a building envelope. Phase lag and amplitude are the two parameters of the frequency characteristics. Therefore, it is necessary to find the optimal values of individual resistances and capacitances of the simplified 3R2C models, which allow the phase lags and amplitudes of the simplified model match that of heat transfer through the real system of a building envelope within the frequency range concerned the best. The objective function of such optimization is expressed in Eq. (29). The optimization is actually searching the optimal values of the five model parameters, which allow the frequency response of the simplified model best fit the theoretical response.

$$J_{\text{3R2C}}(R_1, R_5, C_4) = \sum_{n=1}^{N} \sum_{m=X,Y,Z} \left(W_m^{\text{AM}} \left| |G_m(j\omega_n)| - |G'_m(j\omega_n)| \right| + W_m^{\text{PL}} \times \left| PL\left(G_m(j\omega_n)\right) - PL\left(G'_m(j\omega_n)\right) \right| \right) \tag{29}$$

where, J_{3R2C} is the objective function of the simplified models of the building envelopes, PL is the phase lag (denoted as $PL(G(j\omega))$), N is the number of frequency points, W is the weighting factor associated with the amplitudes and phase lags of frequency characteristics of the external, cross and internal heat conductions, respectively. In this study all the weighting factors were set as 1 as it was found that such value works well. R_1 and R_5 are constrained between 0 and R, which is the total resistance of the construction including air films on both sides. Their sum is less than R. C_4 is constrained between 0 and C, which is the total capacitance of the construction. The other two parameters can be solved as follows:

$$\begin{cases} R_3 = R - R_5 - R_1 \\ C_2 = C - C_4 \end{cases} \tag{30}$$

The number of frequency points N and the frequency range $(10^{-n_1}, 10^{-n_2})$ of concern are determined as follows. n_1, n_2

and N are generally chosen as 8, 3 and $10(n_1 - n_2) + 1$, respectively [21]. With the properties of individual layers of the calculated wall, the theoretical frequency characteristics can be calculated easily. With the assigned parameter values of the simplified models, the frequency characteristics can also be calculated conveniently. A GA estimator used to optimize the parameters is described in Section 5.

4. Parameter optimization for simplified internal mass model

The predicted energy consumption of the simplified building energy model with the differential Eqs. (1)–(7) can be compared with the measured cooling load (Runge–Kutta algorithm is used to solve the equations). The parameters of the simplified building internal mass model are identified using operation data. The optimized parameters are the resistances and capacitances of the building internal mass 2R2C model, which allow the model prediction matches the operation data the best. The objective function for the optimization employs the integrated root-mean-square error of predicted heating/cooling load as defined in Eq. (31).

$$J_{2R2C}(C_{im,1}, R_{im,1}, C_{im,2}, R_{im,2}) = \sqrt{\frac{\sum_{k=1}^{N}(Q_{act,k} - Q_{est,k})^2}{N-1}} \tag{31}$$

where, J_{2R2C} is the objective function of the simplified model of the building internal mass, Q_{act} and Q_{est} are the actual measured and model predicted cooling/heating loads respectively, $C_{im,1}$, $R_{im,1}$, $C_{im,2}$, $R_{im,2}$ are the parameters of the 2R2C model. This is a typical nonlinear optimization problem. Another GA estimator is used to optimize the parameters as described in the next section.

The measured cooling/heating load is calculated using *the return and supply water temperature difference and the water flow rate* retrieved from BMS. To predict the building cooling/heating load using the simplified building energy model, *indoor air temperature and humidity, outdoor air temperature and humidity, fresh air flow rate, solar radiation, occupancy and internal gains* are needed. The means to collect these data for the parameter identification of the internal mass are described in Section 6.

5. GA estimators for parameter optimization of simplified models

Searching for the optimal values of individual resistances and capacitances of the simplified models of the building envelopes and the building internal mass is a nonlinear optimization process. There exist many methods for such optimization problems such as the sequential quadratic programming [22] and the conjugate gradient method [23]. Genetic algorithm (GA) is a better optimization method [15]. It can quickly find a sufficiently good solution. The algorithm was ever used to search for global optimal solutions in HVAC field [24,25]. In this study, GA is also utilized to search for optimal values of individual resistances and capacitance of simplified models of the building envelopes and the simplified model of the building internal mass by minimizing their objective functions.

Fig. 3(a) shows schematically the GA estimator for parameter optimization of simplified models of the building envelopes (3R2C models). It starts with random estimates of the individual capacitances and resistances. The component with largest rectangle represents a GA *run*. Multiple *runs* are allowed. Eq. (32) represents the fitness function (f_{3R2C}) for 3R2C models, which is the reciprocal of the objective function of the minimization problem as Eq. (29).

$$f_{3R2C}(R_1, R_5, C_4) = \frac{1}{J_{3R2C}(R_1, R_5, C_4)} \tag{32}$$

In the genetic algorithm, the three parameters (R_1, R_5, C_4) constitute the chromosome of an individual. The search spaces for (R_1, R_5) are between 0 and the total resistance R, and their sum should less than R. The search space for C_4 is between 0 and the total capacitance C. Initializing the three parameters produces the initial population to start a GA *run*. After the crossover and mutation processes, the next generation population is produced and the fitness is evaluated. The criterion to stop the GA estimator is based on the comparison of the best fitness values of two consecutive *runs*. The GA estimator stops when the relative difference between the two maximum fitness values reaches a threshold value. A GA *run* is also terminated if the number of the current generation is equal to a predefined maximum number.

When the simplified models of the building envelopes are established using the above GA estimator, the parameters of the 2R2C model of the building internal mass can be identified using short-term operation data. Fig. 3(b) shows schematically the GA estimator for parameter optimization of the simplified model of the building internal mass (2R2C model). The fitness function (f_{2R2C}) for the simplified model of the building internal mass, which is the reciprocal of the objective function of the minimization problem as Eq. (31), is represented by Eq. (33).

$$f_{2R2C}(C_{im,1}, R_{im,1}, C_{im,2}, R_{im,2}) = \frac{1}{J_{2R2C}(C_{im,1}, R_{im,1}, C_{im,2}, R_{im,2})} \tag{33}$$

The process of the GA estimator for the 2R2C model is similar to that for the 3R3C models. The GA estimators for parameter identification of these simplified models are developed based on the GA driver by Carroll [26]. The parameters of the GA driver are important for convergence speed. They are selected according to Carroll's recommendation and determined by simulation tests.

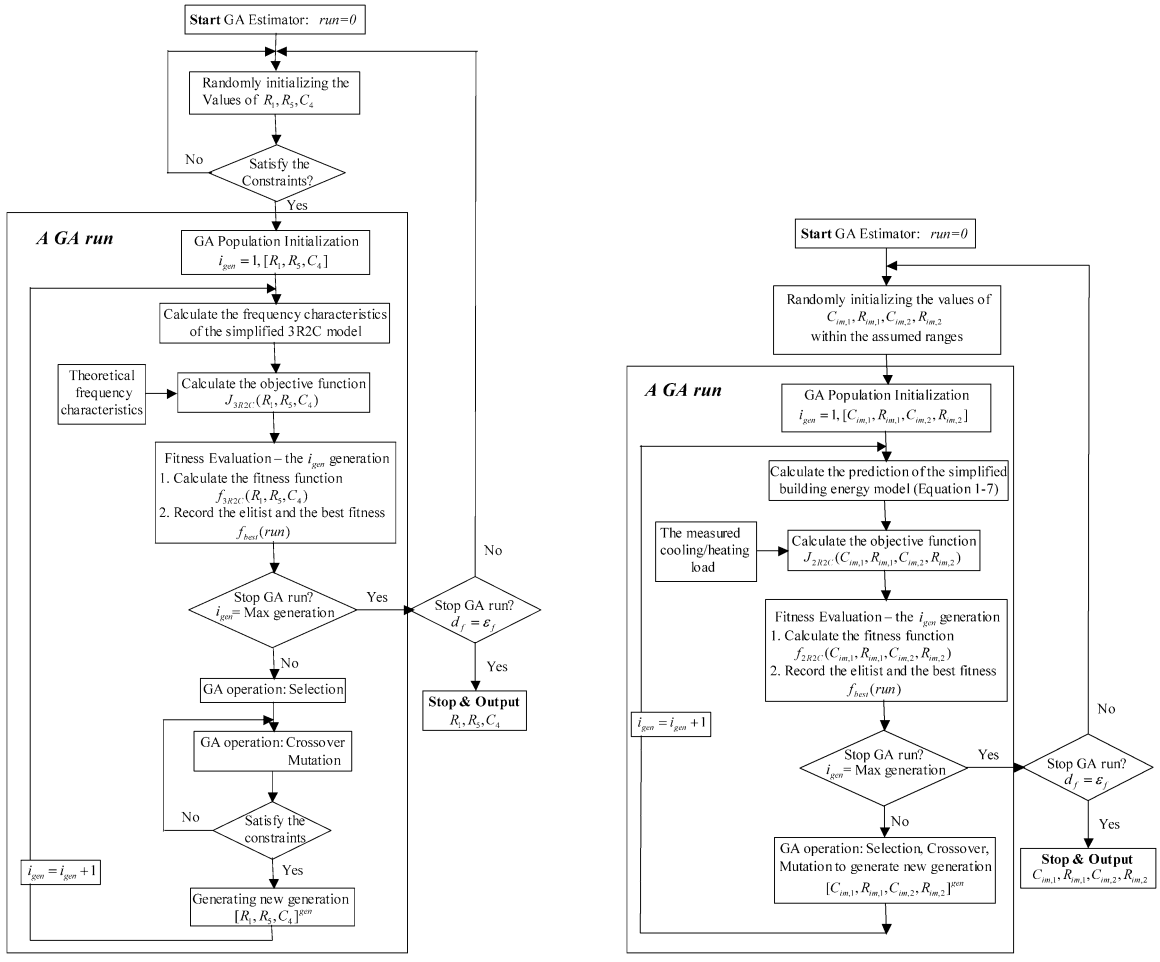

Fig. 3. GA estimators for parameter optimization. (a) For 3R2C models; (b) For 2R2C model.

6. Building system description and data collection

The simplified building dynamic energy model and parameter identification are validated in a real building. The building system description and simplification measures as well as data collection are briefed below.

6.1. Building system and simplification

The building in this study is located in Hong Kong Island and it was completed in 1983. The building consists of a main building of 50 floors with 180 meters high and an attached building of 7 floors with about 28 meters high and a basement of 3 floors. For the main building, the first and second floors are served as shopping centers. The third, fourth and fifth floors are restaurants. The sixth floor is used for chiller plant. The commercial offices are located from the 7th to 49th floors with 2262 m^2 (58×39 m) per floor except that the 15th, 31st, 48th floors are for refuge use. The offices are 3.35 meter high. The 50th floor is used for banquet hall with 6 meter high. For the attached building, the first and second floors are also served as shopping center. The other floors are mainly used for offices with 1738 m^2 (22×79 m) per floor, and the roof is covered with a swimming pool. The basements are used as garage.

The whole building is constructed primarily of heavy weight steel concrete with vertical transportation systems and AHU plants in the core. The external walls are mainly a multilayer construction consisting of 5 layers of homogeneous materials including 300 mm high density concrete between 13 mm face brick and about 13 mm plaster with outside and inside air films. The overall coefficient of heat transfer (U_0) of the windows is about 6.42 $W \cdot m^{-2} \cdot K^{-1}$) with 3.2 mm clean glass as the single glazing material. The floors are 150 mm high density concrete with an about 50 mm refurbishment layer. The ratio of window to wall of the building is approximately 25%. The office ceiling height is about 2.6 meter high. Therefore, 75% of the building volume is used to calculate the indoor air capacity of the building.

The building is air-conditioned with the chiller water plant on the 6th floor except the banquet hall on the 50th floor which is supplied by a separate air-cooled package unit, and the basements which are not air-conditioned. Most of the

air conditioning terminals are AHUs located in the core areas.

For convenience of modeling, the following simplification measures are assumed: (1) The refuge floors are open space. The heat transfer from the refuge floors to the adjacent floors is calculated through the density concrete structure of 150 mm with the simplified 3R2C model; (2) The ceiling of the 49th floor is considered as adiabatic because the 50th floor is air conditioned with a separate unit; (3) The ceiling of the 7th floor of the attached building is also considered as adiabatic because the roof is covered with a swimming pool; (4) The ground floor is merged into building internal mass without special considerations.

6.2. *Data collection and processing*

A site survey was conducted and original design information was collected to build the complete profiles of the occupancy and the use of lighting and equipments. The occupancy load and the internal load from lighting and equipments were estimated according to the rules established on the basis of site survey and according to a previous research on Hong Kong buildings [27] as briefed in the following. The normal occupancy period of office, shopping center and restaurant is from 8:00 am to 6:00 pm, from 10:30 am to 10 pm, and from 6:30 am to 10 pm or late, respectively. The densities of occupancy for the three places are approximately 9, 4.5 and 2 m^2 per person, respectively. The design equipment powers for the three places are 25, 30 and 55 $W{\cdot}m^{-2}$, respectively. The design lighting powers for the three places are 25, 70 and 35 $W{\cdot}m^{-2}$ respectively. The normal patterns of occupancy, equipment power and lighting power are shown in Fig. 4 (occupancy load, light power and equipment power pattern are in factions of their respective peak values). The internal gain from occupancy, lighting and equipments can be split into convective and radiative components according to the recommendations by ASHRAE [28]. For occupancy heat gains, latent heat, convective heat and radiant heat contribute 40%, 20% and 40% respectively.

The offices, shopping centers and restaurants are supplied with fixed amount of fresh air with the ventilation rate of 10, 7 and 7 $L{\cdot}s^{-1}$ per person in the occupancy periods. The return air temperature of AHUs and actual cooling load of the chiller plant were measured and recorded by BMS. The outdoor air temperature and humidity were measured by BMS as well. An average return temperature was taken as the uniform indoor air temperature. Solar radiation cannot be measured directly at the site. Instead, the horizontal global solar radiation was obtained from Hong Kong Royal Observatory. It was decomposed into direct normal solar radiation and diffusive solar radiation with the relationship established by Lam and Li [29] for Hong Kong. The direct normal solar radiation and diffuse solar radiation were used to calculate "solar air temperature" on different external wall surfaces and the solar radiation transmitted through windows.

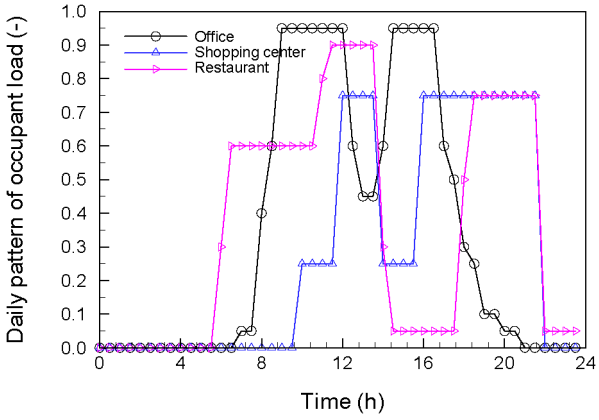

(a)

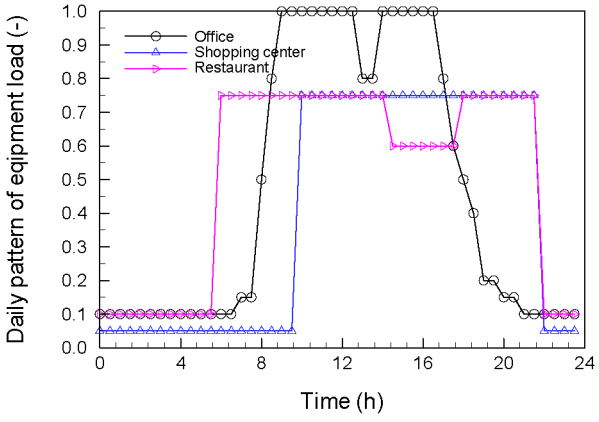

(b)

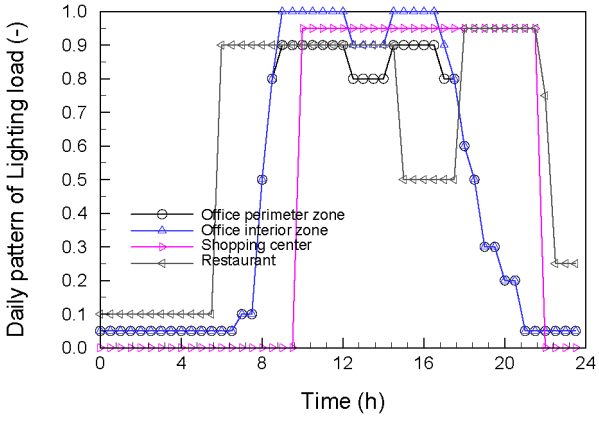

(c)

Fig. 4. Normal patterns of occupancy load, equipment power load and lighting power load. (a) Occupant load profile; (b) Equipment load profile; (c) Lighting load profile.

7. Validation tests and test results

The simplified building energy model was validated using operation data from the real building system described above. The simplified building energy model consists of the simplified models of the building envelopes and the simplified model of the building internal mass. Therefore, the validation process includes three parts: validation of opti-

Table 1
Details and CTF coefficients of a brick/cavity wall of medium construction

Description	Thickness and thermal properties					
	L [mm]	λ [W·m^{-1}·K^{-1}]	ρ [kg·m^{-3}]	C_P [J·kg^{-1}·K^{-1}]	R [m^2·K·W^{-1}]	
Outside surface film					0.060	
Brickwork	105	0.840	1700	800	0.125	
Cavity					0.180	
Heavyweight concrete	100	1.630	2300	1000	0.06135	
Inside surface film					0.120	
k	0	1	2	3	4	5
b_k [W·m^{-2}·K^{-1}]	0.000179	0.013915	0.043460	0.018036	0.001034	0.000005
c_k [W·m^{-2}·K^{-1}]	6.953625	−12.223156	5.985915	−0.660046	0.020334	−0.000044
d_k	1.000000	−1.620834	0.726131	−0.065025	0.001594	0.000000

Table 2
Parameters of simplified 3R2C models of a brick/cavity wall

Model	Parameters of resistance and capacitance R [m^2·K·W^{-1}], C [J·m^{-2}·K^{-1}]						
	R_1	C_2	R_3	C_4	R_5	R (total)	C (total)
Theoretical model	–	–	–	–	–	0.5455	372800
Simplified model (a)	0.0586	186400	0.3663	186400	0.1206	0.5455	372800
Simplified model (b)	0.1818	186400	0.1818	186400	0.1818	0.5455	372800
Optimal simplified model	0.0929	122420	0.3111	250380	0.1415	0.5455	372800

mal nodal placement of the simplified models of the building envelopes with GA estimator (Section 7.1), parameter identification of the simplified model of the building internal mass (Section 7.2), validation of the simplified building energy model in different operation conditions (Section 7.3).

7.1. Validation of the simplified models of the building envelopes

To validate the effectiveness and accuracy of the GA-based optimal nodal placement for the simplified models of the building envelopes, the outputs of the 3R2C model with optimal nodal placement are compared with that of the theoretical model and two simplified 3R2C models (as reference models) with typical configurations normally used in practical applications [12,14], in frequency domain and time domain. The two reference models are namely model (a) and model (b) in this paper. For model (a) the three resistances take the values of the outside conductive resistance, wall conduction resistance and inside conductive resistance respectively, the value of individual capacitance is half of the total capacitance. For model (b), the three resistances and two capacitances are distributed evenly.

Many case studies were conducted to validate the optimal nodal placement method for the simplified building models and the accuracy of the simplified models. One case for a brick/cavity wall (details are given in Table 1) is presented in this paper. This wall is often used to validate various calculation methods [21,30]. Its CTF coefficients provide a convenient reference to calculate the transient thermal transfer of the theoretical model with variable sol-air temperature and indoor air temperature. With GA estimator, the optimal parameters of the model (i.e., simplified model with optimal nodal placement) were obtained. The parameters of the three simplified models are shown in Table 2.

Because the heat transfer into indoor space is directly related to the frequency characteristics of the cross heat conduction and internal conduction of the building envelopes, only these frequency characteristics were displayed for comparison and validation. The frequency responses of the four models have similar characteristics in the low frequency region as shown in Figs. 5 and 6. The frequency range presented in the figure is the range normally concerned for building dynamic simulation. For the frequency response characteristics of the cross heat conduction, Fig. 5(a) shows that the amplitudes of the simplified model with optimal nodal placement almost overlap with that of the theoretical model, while the amplitudes of the simplified model (a) are greater than that of the theoretical model and the amplitudes of simplified model (b) are less than that of the theoretical model in the high frequency region. Fig. 5(b) indicates that the three simplified models have similar phase lags deviating from the theoretical phase lag in the high frequency region. For the frequency response characteristics of the internal heat conduction, Figs. 6(a) and 6(b) indicate that the amplitudes and phase lags of the simplified model with optimal nodal placement (i.e., optimal simplified model) agree well with that of the theoretical model while the frequency characteristics of simplified models (a) and (b) deviate significantly from the theoretical frequency characteristics in the high frequency region. The simplified model with optimal nodal placement performs obviously better than the models with other configurations do. The same result can be observed when comparing the calculated heat gains of those models as presented later.

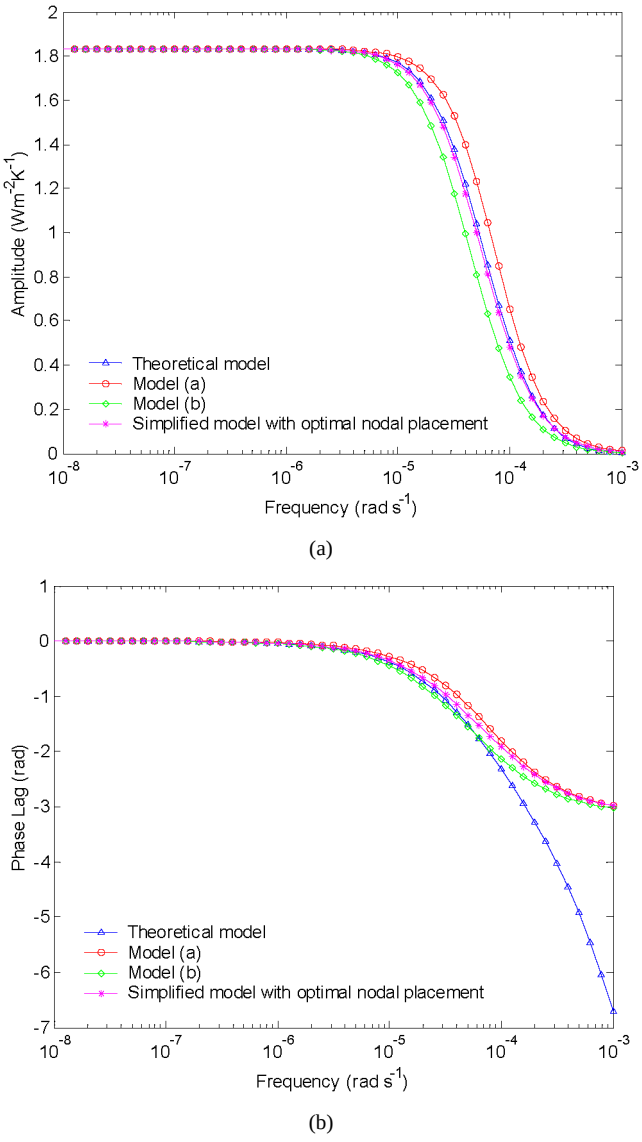

Fig. 5. Frequency responses of cross heat conduction for Brick/cavity wall. (a) Amplitude; (b) Phase lag.

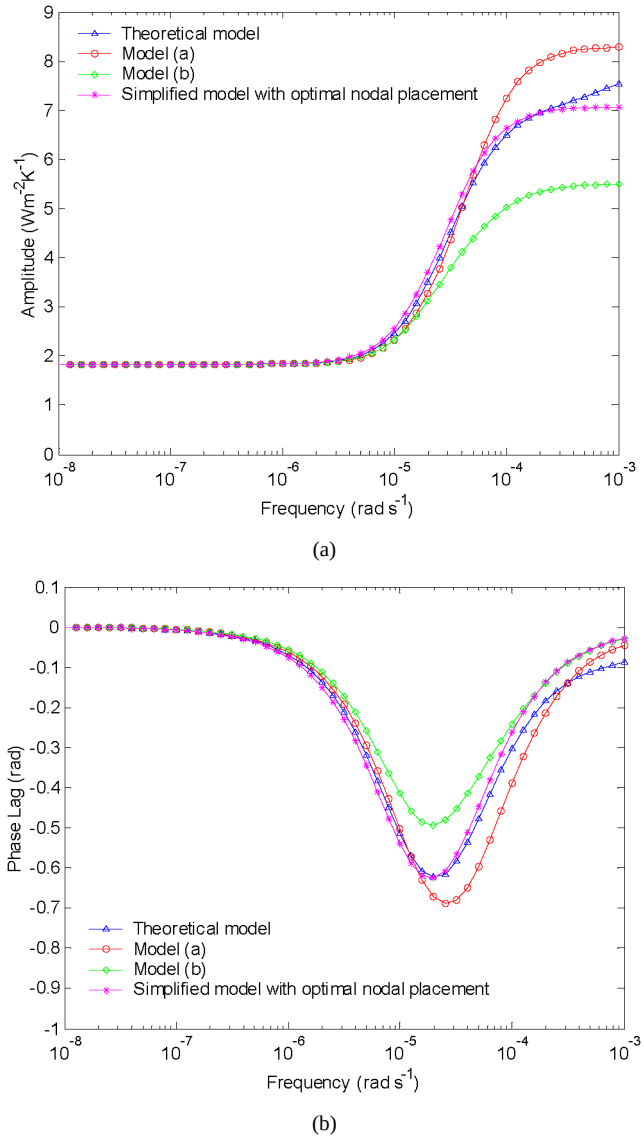

Fig. 6. Frequency responses of internal heat conduction for Brick/cavity wall. (a) Amplitude; (b) Phase lag.

In real applications, the indoor air temperature changes continuously. Therefore, it is necessary to consider the effects of the change of indoor air temperature. For an intermittent air-conditioned building with the brick/cavity external wall, the daily sol-air temperature and indoor air temperature in a typical summer day are selected for heat gain estimation as shown in Fig. 7. The heat gains of the simplified models are calculated using the parameters listed in Table 2 while the heat gain of the theoretical model is calculated using CTF method with the coefficients listed in Table 1.

The heat gains of these simplified models are compared with that of the theoretical model as shown in Fig. 8. The average absolute errors (namely, percent average absolute error) of hourly heat gains of Model (a), Model (b) and the simplified model of optimal nodal placement (compared with that of the theoretical model) are 6.1%, 10.7% and 3.4% respectively. These results further confirm again that the simplified model with optimal nodal placement agrees better with the theoretical model when compared with other simplified models. The average absolute error is used in this paper because it can reflect the deviation of predicted values from the theoretical values or measurements more clear and accurate than the absolute error.

7.2. Parameter estimation of the simplified model of the building internal mass

After the optimal nodal placement of the simplified models of the building envelopes was achieved using the GA estimator as described above, the parameters of the building internal mass model were then identified using the other GA estimator. In this process, the operation data were used for

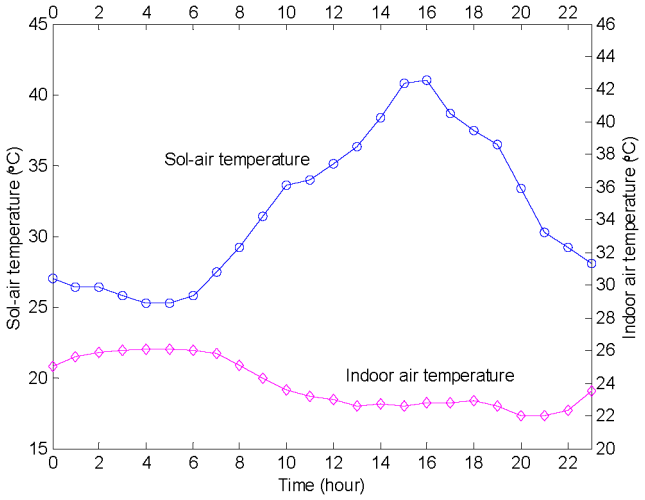

Fig. 7. Profiles of sol-air temperature and indoor air temperature.

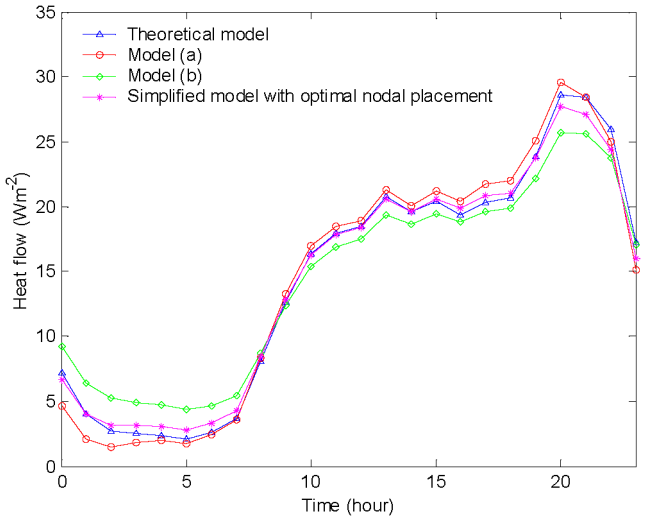

Fig. 8. Hourly heat gains through the brick/cavity wall.

model prediction. The parameter identification of the internal mass model is achieved actually by searching the values of the 2R2C, which allow the predicted building cooling load best fits the measured cooling load.

For the building concerned, the basic structure of the floor layer is density concrete of 150 mm. Because the internal mass includes the basic structure of the floor layer, the partitions, the internal walls, and furniture, etc., the searching scopes of the parameters of the building internal mass with GA estimator should be much larger than the capacitance and resistance of the basic structure of the floor layer. The searching scope of both resistances was assumed between zero and the sum of resistances of the indoor air film and three times the resistance of the floor basic structure. The searching scope of both capacitances was assumed between zero and three times the capacitance of the floor basic structure.

The operation data of the building for consecutive fourteen days (two weeks) in typical summer season were used

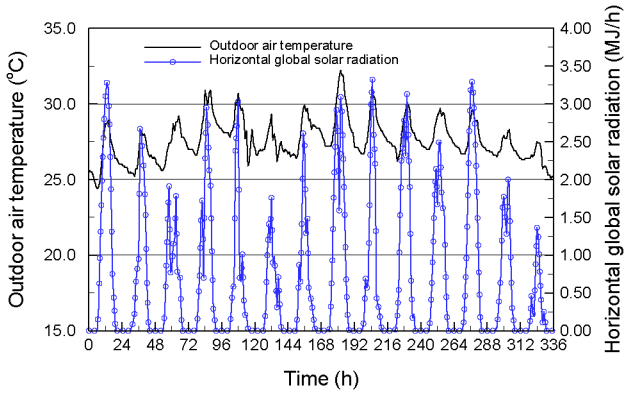

Fig. 9. Outdoor air temperature and horizontal global solar radiation (parameter identification case).

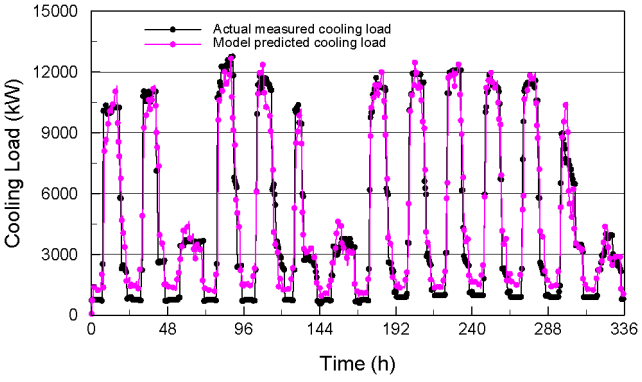

Fig. 10. Actual measured cooling load *vs* model predicted cooling load (parameter identification case).

to identify the parameters of the 2R2C building internal mass model. The outdoor air temperature and horizontal global solar radiation for the parameter identification case are shown in Fig. 9. Most of the days were sunny and cloudy, and the others were sunny with a few showers.

The air-conditioning systems in offices operated in the office hours between 8:00 pm and 18:00 pm. The air conditioning systems in restaurants and shopping centers were shut down a little later. Almost each office floor has fan coil units to supply cooling load to communication or computation rooms for non-office hours such as night-time and holidays. The cooling load in these hours was only a very small part of the total building cooling load in the normal office hours. The temperatures measured in non-office hours cannot represent the indoor air temperature because the sensors installed in air chamber (in the core of the building) and the air in offices is stagnant. Therefore, only the operation data in office hours were used to identify the parameters of building internal mass model. It is worth noticing that the operation data in non-office hours are preferably used in the fittings for parameter identification when reliable measurements in that period are available.

The identified parameters using GA estimator are: $C_{\mathrm{im},1} = 648729\ \mathrm{J{\cdot}m^{-2}{\cdot}K^{-1}}$, $C_{\mathrm{im},2} = 73793\ \mathrm{J{\cdot}m^{-2}{\cdot}K^{-1}}$, $R_{\mathrm{im},1} = 0.299\ \mathrm{m^2{\cdot}K{\cdot}W^{-1}}$, $R_{\mathrm{im},2} = 0.0282\ \mathrm{m^2{\cdot}K{\cdot}W^{-1}}$.

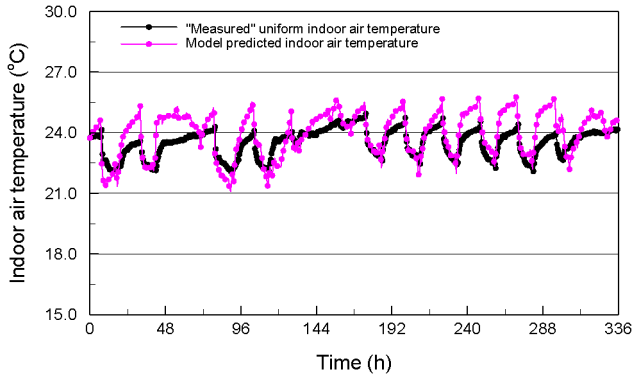

Fig. 11. "Measured" uniform indoor air temperature *vs* model predicted indoor air temperature (parameter identification case).

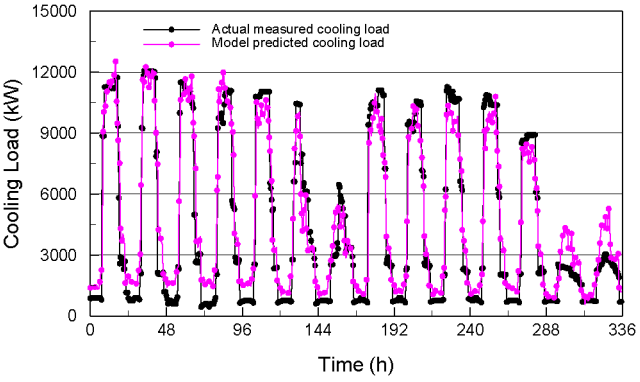

Fig. 12. Actual measured cooling load *vs* model predicted cooling load (validation–summer case).

Fig. 10 presents model predicted cooling load with the identified parameters of the building internal mass model against the actual measured cooling load. The average absolute error was 7.8% for the data points of office hours between 8:00 am and 8:00 pm. Fig. 11 presents the model predicted uniform indoor air temperature with the identified parameters of the building internal mass model and the measured cooling load in the period used for parameter identification. It shows that the identified model could well predict the trends of indoor air temperature. Comparisons show that the model predicted indoor air temperature in the office hours well agreed with the "measured" uniform indoor air temperature.

7.3. Validation of the simplified building energy model

To further validate the simplified building energy model developed, it was used to predict the cooling load with the "measured" uniform indoor air temperature in other two operation periods. One was also in summer season lasting for two weeks, and the other was in winter season lasting for one week. The same building model was also used to predict the uniform indoor air temperature with the given cooling load in the "reverse direction". The internal heat gains used were the same in both cases.

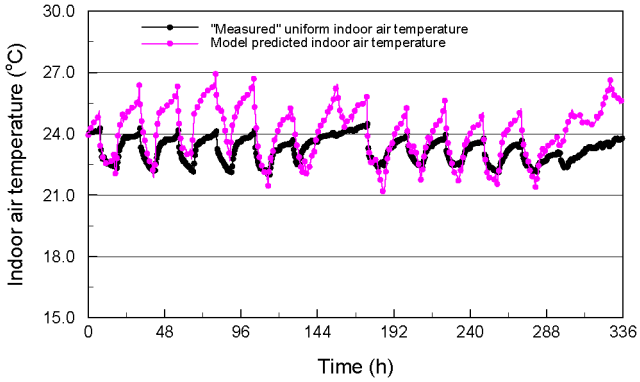

Fig. 13. "Measured" uniform indoor air temperature *vs* model predicted indoor air temperature (validation–summer case).

In the summer case, the weather condition was similar to that used for the training process as shown in Fig. 9. Fig. 12 presents the model predicted cooling load profile using the building model compared with the actual measured cooling load profile. It shows that the model can dynamically predict cooling load, which agreed well with the actual measured cooling load. The model predicted cooling load could follow the trends of energy consumption accurately. The average absolute error between predicted and measured cooling load was 9.7% when the data points in non-office hours were excluded. If all the data points including that in office hours and non-office hours, were used for model validation, the error was higher, 22.2%. It is observed that the model trended to over-predict cooling load for non-office hours due to the fact that measured return air temperature measurement in non-office hours was not a reliable indicator and was significantly lower than the true average air temperature in the building. This point can be explained in more detail as follows.

Fig. 13 presents the model predicted uniform indoor air temperature (using the measured cooling load) compared with the "measured" indoor air temperature in the summer case. The "measured" indoor air temperature was the average of the measured return air temperatures. It shows that the model can predict the trends of indoor air temperature correctly. At the beginning of office hours, the indoor air was cooled down by air handling systems. In contrast, when air handling systems were shut down in non-office hours (at night and weekend days), the indoor air was warmed up by heat transfer through building envelopes and heat transfer of the building internal mass. Comparison shows that the model predicted indoor air temperature in the office hours agreed well with the "measured" uniform indoor air temperature. In non-office hours, the model predicted indoor air temperature was significantly higher than the "measured" uniform indoor air temperature. It is because, in office hours, the air was circulating and the measured return air temperature in the return air chamber could well represent the indoor air temperature. However, in non-office hours, the measured return air temperature was obviously lower than the real indoor air temperatures in summer season because the air was stag-

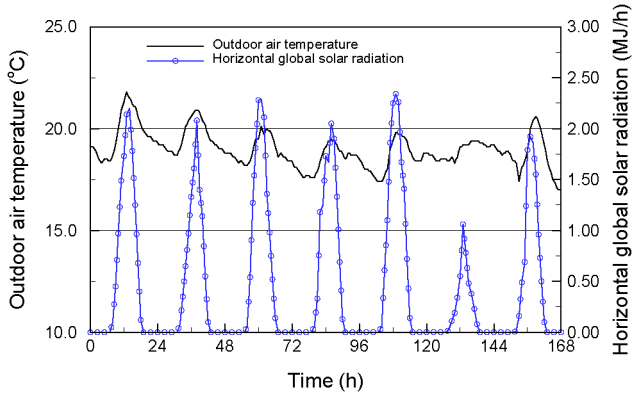

Fig. 14. Outdoor air temperature and horizontal global solar radiation (validation–winter case).

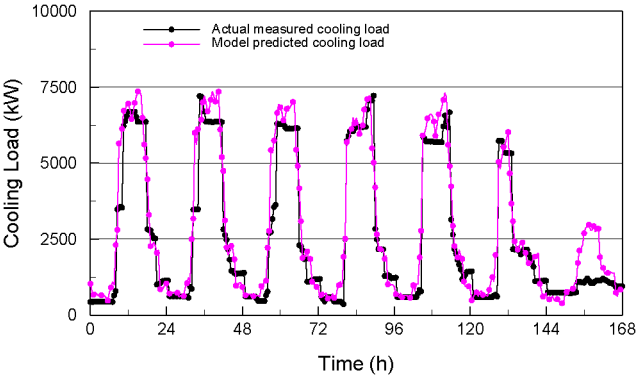

Fig. 15. Actual measured cooling load *vs* model predicted cooling load (validation–winter case).

nant and the measured return air temperature in the return air chamber (in core area) was not affected (i.e. heated up) significantly by the outside weather condition. Therefore, the model predicted indoor air temperature could represent the uniform indoor air temperature more accurately compared with the "measured" uniform indoor air temperature in non-office hours.

The building model was also validated with a week long operation data in a winter case which was a very different operating condition. Fig. 14 shows the outdoor air temperature profile and horizontal global solar radiation profile. The outdoor air temperature was much lower than that in summer season. Most of the days were sunny and the intensities of the solar radiation were lower than that used for model training. Fig. 15 presents the actual measured cooling load and model predicted cooling load. The model predicted cooling load agreed with the actual measured cooling load in office hour with a corresponding average absolute error of 12.0%.

In summary, the simplified building energy model can predict the thermal performance of building system such as energy consumption and indoor air temperature for practical applications with acceptable accuracy. It has extensive applicability under different operation conditions by capturing the dynamic characteristics of building system correctly.

8. Conclusion

Simplified building energy models, which can reliably predict the dynamic thermal performance of the building system, are highly desirable for performance evaluation and diagnosis etc. However, it is a great challenge to represent the thermal characteristics of the building system with simplified models for either building envelopes or the building internal mass. Estimation of model parameters is essential when using simplified model in applications. Studies show it is feasible to develop simplified models of the building system to predict dynamic thermal performance of good accuracy.

An efficient and effective method for parameter estimation of the simplified models is important in practical application. This paper presented a method to simplify building thermal system and to estimate the parameters of the simplified model. The simplified building energy model consists of the simplified models of the building envelopes and the simplified model of the building internal mass. The parameters of the simplified models of the building envelopes are identified using easily available physical properties based on the frequency response characteristic analysis. The parameters of the building internal mass model are identified using monitored operation data. Genetic algorithm (GA) provides an efficient means for the nonlinear parameter optimization in parameter identification.

Test results in a real commercial office building with different operation conditions demonstrated that the simplified building energy model can predict the dynamic thermal performance of the building robustly and accurately. The model predicted cooling load shows the average error was about ten percent compared to the actual measured cooling load. The model can also well predict average indoor air temperature. The robustness of the model to predict the thermal performance owes to that the model represents the dynamic characteristics of the building system physically and the model parameters are partially determined using the building physical properties. At the same time, the accuracy of the simplified model owes partially to that part of the model parameters are identified using the actual monitored operation data by best fitting the model outputs with the operation data. The model can provide thermal performance prediction of good accuracy and robustness for practical applications.

Acknowledgement

The research work presented in this paper is financially supported by a grant from the Research Grants Council (RGC) of the Hong Kong SAR and a research grant of The Hong Kong Polytechnic University.

References

[1] J. House, G. Kelly, (NIST). An overview of building diagnostic, http://poet.lbl.gov/diag-workshop/proceedings, 1999.

[2] M. Liu, L. Song, D. Claridge, et al., Development of whole-building fault detection methods, http://buildings.lbl.gov/hpcbs/pubs/E5P23T1c.pdf, 2002.

[3] J. Braun, K. Montgomery, et al., Evaluating the performance of building thermal mass control strategies, HVAC&R Res. 7 (4) (2001) 403–428.

[4] G. Henze, C. Felsmann, G. Knabe, Evaluation of optimal control for active and passive building thermal storage, Int. J. Thermal Sci. 43 (2) (2004) 173–183.

[5] Y. Yao, Z. Lian, S. Liu, et al., Hourly cooling load prediction by a combined forecasting model based on Analytic Hierarchy Process, Int. J. Thermal Sci. 43 (11) (2004) 1107–1118.

[6] D. Crawley, L. Lawrie, C. Pedersen, et al., EnergyPlus: Energy simulation program, ASHRAE J. 42 (4) (2000) 49–56.

[7] DOE-2 Engineering Manual, Version 2.1C, Lawrence Berkeley Laboratory, Berkeley, CA, 1982.

[8] M. Liu, D. Claridge, N. Bensouda, et al., Manual of procedures for calibrating simulations of building systems, http://buildings.lbl.gov/hpcbs/Element_5/02_E5_P2_3_2.html, 2003.

[9] K. Minoru, D. Charles, et al., Hourly thermal load prediction for the next 24 hours by ARIMA, EWMA, LR and an artificial neural network, ASHRAE Trans. 101 (1) (1995) 186–200.

[10] S. Kalogirou, C. Neocleous, et al., Heating load estimation using artificial neural networks, In: Proc. CLIMA 2000 Conf., Brussels, Belgium, 1997.

[11] A. Dhar, T. Reddy, et al., A Fourier series model to predict hourly heating and cooling energy use in commercial buildings with outdoor temperature as the only weather variable, J. Solar Energy Engrg. 121 (1999) 47–53.

[12] K. Braun, N. Chaturvedi, An inverse gray-box model for transient building load prediction, HVAC&R Res. 8 (1) (2002) 73–99.

[13] Z. Liao, A. Dexter, A simplified physical model for estimating the average air temperature in multi-zone heating systems, Building and Environment 39 (2004) 1013–1022.

[14] J. Seem, S. Klein, et al., Transfer functions for efficient calculation of multidimensional transient heat transfer, J. Heat Transfer 111 (1989) 5–12.

[15] M. Mitchell, An Introduction to Genetic Algorithm, MIT Press, Cambridge, MA, 1997.

[16] T. Kusuda, Thermal response factors for multilayer structures of various heat conduction systems, ASHRAE Trans. 75 (1969) 246–271.

[17] K. Ouyang, F. Haghighat, A procedure for calculating thermal response factors of multilayer walls—state space method, Building and Environment 26 (2) (1991) 173–177.

[18] M. Ciampi, F. Leccese, G. Tuoni, Multi-layered walls design to optimize building-plant interaction, Int. J. Thermal Sci. 43 (4) (2004) 417–429.

[19] Y.M. Chen, Z.K. Chen, A neural-network-based experimental technique for determining z-transfer function coefficients of a building envelope, Building and Environment 35 (2000) 181–189.

[20] C.T. Chen, System and Signal Analysis, second ed., Saunder College Publishing, USA, 1994.

[21] S.W. Wang, Y.M. Chen, A novel and simple building load calculation model for building and system dynamic simulation, Appl. Thermal Engrg. 21 (2001) 683–702.

[22] J. House, T. Smith, Optimal control of a thermal system, ASHRAE Trans. 97 (2) (1991) 991–1001.

[23] J. Nizet, L. Lecomte, F. Litt, Optimal control applied to air conditioning in building, ASHRAE Trans. B 90 (1) (1984) 587–600.

[24] S.W. Wang, X.Q. Jin, Model-based optimal control of VAV air-conditioning system using genetic algorithm, Building and Environment 35 (6) (2000) 471–487.

[25] S.W. Wang, J.B. Wang, Robust sensor fault diagnosis and validation in HVAC systems, Trans. Inst. Measurement Control 24 (3) (2002) 231–262.

[26] D.L. Carroll, FORTRAN Genetic algorithm (GA) driver, Version 1.7a, http://cuaerospace.com/carroll/ga.html, http://cuaerospace.com/carroll/gatips.html, 2001.

[27] An environmental assessment for new building developments, HK-BEAM, Version 2003, HK-BEAM Society, Kowloon, Hong Kong, 2003.

[28] Handbook of Fundamentals, American Society of Heating, Refrigerating and Air-Conditioning Engineers, Atlanta, USA, 1997.

[29] C. Lam, H.W. Li, Correlation between global solar radiation and its direct and diffuse components, Building and Environment 31 (6) (1996) 527–535.

[30] M.G. Davies, A time-domain estimation of wall conduction transfer function coefficients, ASHARE Trans. 102 (1) (1996) 328–343.